Technical University of Denmark

DTU

Application of lidars for assessment of wind conditions on a bridge site

Jakobsen, J. B.; Cheynet, Etienne ; Snæbjörnsson, Jonas ; Mikkelsen, Torben Krogh; Sjöholm, Mikael; Angelou, Nikolas; Hansen, Per; Mann, Jakob; Svardal, Benny ; Kumer, Valerie ; Reuder, Joachim

Link back to DTU Orbit

DTU Library
Technical Information Center of Denmark

Application of lidars for assessment of wind conditions on a bridge site

Jasna Bogunović Jakobsen[1], Etienne Cheynet[1], Jonas Snæbjörnsson[1,2], Torben Mikkelsen[3], Mikael Sjöholm[3], Nikolas Angelou[3], Per Hansen[3], Jakob Mann[3], Benny Svardal[4], Valerie Kumer[5] and Joachim Reuder[5]

[1]Department of Mechanical and Structural Engineering and Materials Science, University of Stavanger, Norway
[2]School of Science and Engineering, Reykjavik University, Iceland
[3]Department of Wind Energy, Risø campus, Technical University of Denmark, Denmark
[4]Christian Michelsen Research, Bergen, Norway
[5]Geophysics Institute, University of Bergen, Norway
email: jasna.b.jakobsen@uis.no, etienne.cheynet@uis.no, jonasthor@ru.is, tomi@dtu.dk, misj@dtu.dk, nang@dtu.dk, perh@dtu.dk, jmsq@dtu.dk, benny.svardal@cmr.no, valerie.kumer@gfi.uib.bo, joachim.reuder@gfi.uib.no

ABSTRACT: Wind measurement techniques based on remote optical sensing, extensively applied in wind energy, have been exploited in civil engineering only in a limited number of studies. The present paper introduces a novel application of wind lidars in bridge engineering, and presents the findings from the pilot measurement campaign on the Lysefjord Bridge in the South-West Norway. A single long-range pulsed WindScanner lidar and two short-range continuous-wave WindScanner lidars were deployed, in addition to five sonic anemometers installed on the bridge itself, the latter for long-term wind characterization. The paper presents a promising comparison of the measurements obtained by the three different sets of instruments, and discusses their complementary value.

KEY WORDS: ICWE14; Sonic Anemometers; Pulsed Doppler Lidar, Short-Range WindScanner, Long-Span Bridge; Turbulence; Wind Spectra, Coherence.

1   INTORDUCTION

1.1   Background

The Norwegian government has adopted an ambitious plan for a ferry-free highway along the 1100 km coastal route South-West in Norway, between Kristiansand and Trondheim [1]. Over a twenty years long period, eight new and challenging fjord crossings are planned for construction. For most of the strait crossings in question, wind loads will be among the governing design factors. In relation to that, various research activities devoted to the assessment of wind conditions and validation of the computational models for wind-induced vibrations have been initiated.

Among them is the measurement campaign on the Lysefjord Bridge in the vicinity of Stavanger, in which complex flow conditions at the Lysefjord inlet are being studied, as well as the associated buffeting response of the bridge. A novel part of the project concerns employment of wind measurement techniques based on remote optical sensing, in parallel with the long-term sonic anemometer measurements. The present investigations were triggered by the recent rapid development of the wind lidar (light detection and ranging) measurement technology and its extensive applications in wind energy for resource and wind condition assessment, including wind turbine induction zone inflow- and wake zone studies and the use of wind lidars for improved wind turbine control, cf. e.g. [2].

In civil engineering, the remote wind sensing techniques have been exploited only in a limited number of studies, focusing on the wind profile and the boundary layer thickness in relation to design wind loads on buildings. In [3], wind conditions up to the 420 m altitude were studied as a function of the upstream fetch roughness, by the simultaneous deployment of two Doppler sodars in the Tokyo area. Similarly, a single Doppler sodar was used to monitor the wind profile up to 210 m height in the urban area of Hanover, and demonstrate its dependency on the surface roughness and the thermal effects [4].

In [5], a pulsed lidar was used to characterize the urban boundary layer in the central part of London. The wind velocity data, extracted from the lidar measurements in the so-called Doppler Beam Swinging mode, were related to the sonic anemometer data at a location nearby, and used to review the analytical models for the wind profiles in urban areas [6].

To the authors' knowledge, the relevance and the potential of scanning Doppler lidars for bridge engineering has not been explored before. Prior to a bridge construction, remote sensing based wind measurements could provide an important link between the local flow conditions, at the very bridge site, and those observed by the wind sensors on a measurement mast in a different flow environment, at a certain distance from the bridge. Related to this, lidars can be utilized to investigate the effects of the

complex terrain on the wind characteristics, such as flow homogeneity along the bridge span. Furthermore, important information on the temporal and spatial characteristics of turbulence along the bridge-span, including coherence, which are all fundamental quantities for bridge design, can be extracted from the remote sensed wind lidar measurements. The present work investigates some of these possibilities utilizing the Lysefjord Bridge for a case study.

1.2 Bridge site characteristics

The Lysefjord Bridge is located at the inlet of a 40 km long fjord, less than 2 km wide and defined by the hills reaching 1000 m in height. At the bridge location, the fjord narrows down to 500-600 m, so that the total bridge length is 600 m and the main span 446 m. The surrounding hills follow the slope of 30-45° and reach 350 m in height to the North and 600 m to the South. Few kilometers South-West of the bridge, the Lysefjord connects to the Høgsfjord, orientated from North-West (NW) to South-East (SE), as the bridge itself. Further to the West, the 20 km of hilly terrain changes into a 10 km wide area of flat coastal terrain. The meteorological station at Stavanger airport at Sola, at the coast, was used as a reference station when establishing the design basis for the bridge. The 10-minutes 50-year mean wind speed is estimated to be 36 m/s at the deck height and the three second gust is 49 m/s [7]. Figure 1 shows the terrain surrounding the bridge.
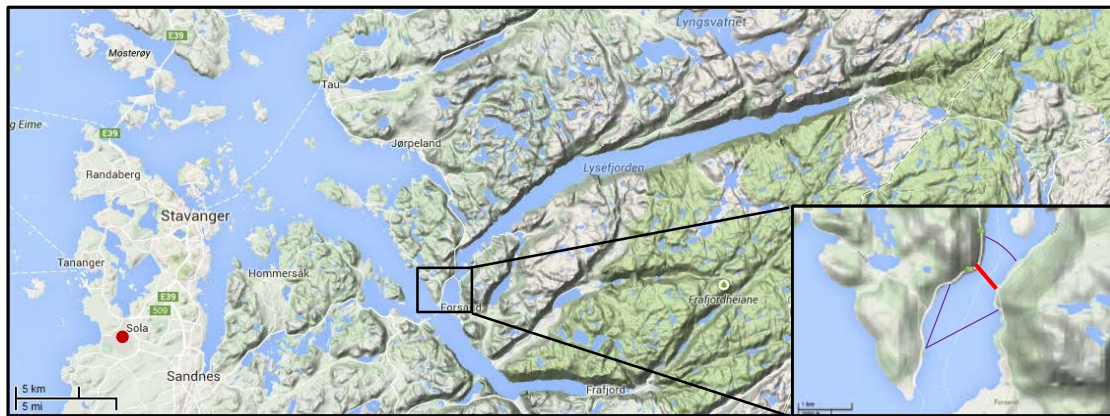

Figure 1. Lysefjord Bridge (red line) situated in mountainous complex terrain, Sola airport (red dot) and the area surveyed by the pulsed lidar (cf. inserted rectangle).

2 WIND VELOCITY MONITORING SYSTEMS

2.1 Long-term wind observation system

Four 3D WindMaster Pro sonic anemometers from Gill Instruments Ltd and one Vaisala weather transmitter WXT520 were mounted on the hangers and the main bridge cable, in November 2013. They were installed from the walkway on the South-West side of the bridge, at distances 96 m, 24 m, 0, -24 m and –72 m from the mid-span, with positive values indicating the position towards North. The sensors are operating approximately 6 m above the bridge deck, which has an elevation of 54.5 m. In July 2014, three additional anemometers were mounted on the bridge, for an expanded long-term monitoring. The wind data is recorded at the rate of 32 Hz by the 3D sonic anemometers and at 4 Hz by the Vaisala sensor. The data is typically organized in 10 minutes records and studied in terms of mean wind speed, turbulence intensity and the (cross-) spectral densities of turbulence. Figure 2 (left) shows a 3D sonic anemometer fixed to the bridge hanger 72 m South-East from the mid-span. Further information on the monitoring system is presented in the companion paper [8].

Figure 2. 3D WindMaster Pro fitted to a bridge hanger (left), WindCube 100S at the Lysefjord Center with the bridge in the background (middle) and one of the two short-range WindScanner lidars (R2D1) at the bridge walkway (right).

2.2 Wind velocity measurements by the long-range scanning pulsed lidar

The lidar measurements were undertaken in two stages. The first phase was performed from March to June 2014, using a WindCube100S, a long-range pulsed Doppler lidar instrument with a steerable, scanning laser beam. The study was supported by the Norwegian Public Road Administration (NPRA) and carried out as a research collaboration between the University of Stavanger, University of Bergen and Christian Michelsen Research, with an in-kind contribution from the French lidar manufacturer Leosphere.

The WindCube 100S lidar was mounted 1.75 km South-West from the bridge, on the North side of the fjord, at an elevation of 5.7 m. Four different scanning modes were applied and experimented with: (i) Doppler Beam Swinging mode (DBS) for wind profile monitoring, (ii) Plan Position Indicator mode (PPI) for scanning over a range of azimuth angles at a fixed elevation, (iii) Range Height Indicator mode (RHI) for observations at a fixed azimuth but varying elevation and the (iv) Sequential Fixed Line of Sight mode (LOS) for measurements along a single line. Figure 3 illustrates the PPI and the RHI scan domains, see also Figure 1.

A typical scanning cycle was set to last for one hour and included the first three modes investigating the flow homogeneity. The PPI mode was applied at three elevations (0.8°, 1.8° and 3.2°), corresponding to 30.2 m, 60.7 m and 103.6 m height at the bridge location. The azimuth sector covered was from 13° to 63° (see Figure 1 and Figure 3, left) in steps of 1° per 0.2 second, giving a resolution of 31 m along the bridge. The radial resolution in this case was 25 m, reaching a maximum scanning distance of 2440 m from the lidar. The RHI scans were recorded at three azimuth angles targeting the bridge main span, for elevations from 0° to 6° in steps of 0.6°, corresponding to a vertical resolution of 18 m at the bridge site (Figure 3, right). The 25 m long range gates overlapped, providing the "resolution" of 10 m in the radial direction. Towards the end of the measurement campaign, over a one week period, the LOS mode with a radial resolution of 10 m, based on the overlapping 25 m long range gates, was implemented, targeting the central part of the bridge span. In the following, only the PPI and the LOS scan data will be discussed.
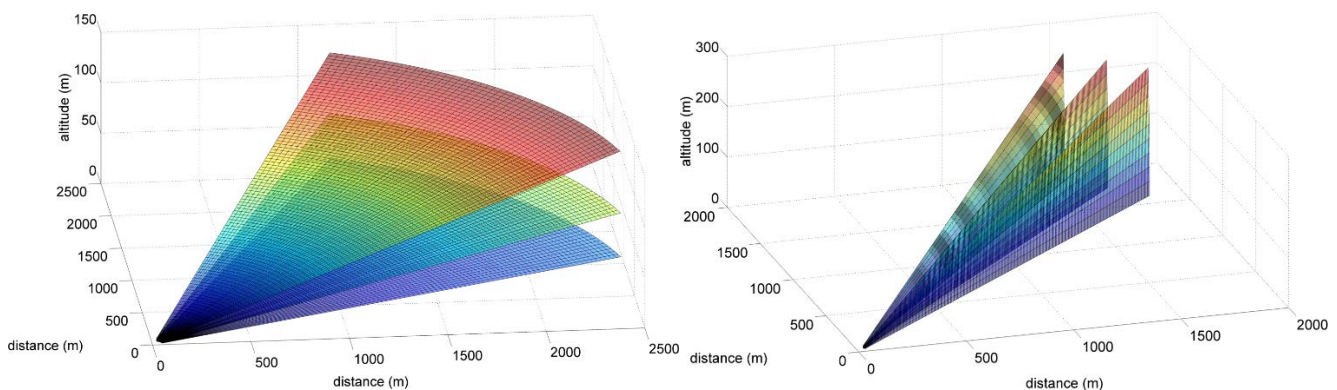

Figure 3. Plan Position Indicator mode scanning domain, elevations 0.8°, 1.8° and 3.2° (left), and the Range Height Indicator mode domain, for azimuth 37 °, 38 ° and 39 ° (right), for the long-range lidar

2.3 Wind flow characterization by two syncronized short-range contineous wave WindScanners

In May 2014, the second phase of the study was carried out as a research collaboration between the Technical University of Denmark (DTU), the University of Stavanger, Christian Michelsen Research and the University of Bergen, with the support from the Norwegian Public Road Administration. Two short-range WindScanners (www.windScanner.dk) developed by DTU Wind Energy, building upon modified ZephIR 150 continuous wave lidars, were deployed on the bridge walkway on the West side (see Figure 2 right). The high temporal and spatial resolution (at short distances) of the continuous wave lidars makes short-range WindScanners particularly suited for studying the wind velocity fluctuations. The scanning sequences were dedicated to the investigation of the characteristics of the inflow, as well as to identifying the footprints of the bridge structure in the flow. The Doppler spectra were averaged such that LOS wind velocities were provided at 390.625 Hz and the scan pattern duty cycle was 1 Hz.

The two short-range high-resolution scanning wind lidars were installed in a central part of the mid-span, with a distance of 90 m between them, and remotely operated and synchronized to monitor the flow in different planes on the South-West side of the bridge. Wind velocity along a 120 m long horizontal line 40 m in front of the bridge deck was surveyed in particular, see Figure 4. The positive directions for the radial velocities in the figure are adapted to the comparison presented in Figure 6, i.e. opposite to the sign convention used when acquiring the data. In this measurement configuration, the measurement distance set by the lidars focal length of the light beam to the line 40 m from the bridge varied between 40 m and 112.4 m. The cw lidars line-of-sight full-width-half-maximum (FWHM) weighting function correspondingly varied between 2 m and 15.9 m, [9].
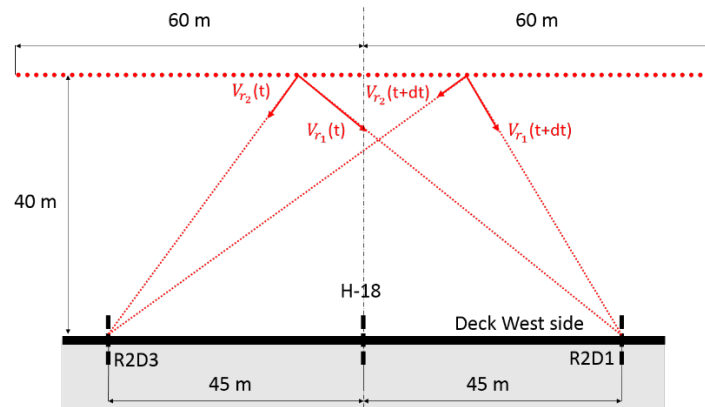
Figure 4. Top view of the main measurement setup with two short-range WindScanners

3 RESULTS

3.1 Wind velocity characteristics observed by a non-scanning, fixed line- of-sight, measurement setup

In the following, the wind velocity data acquired with a non-scanning, fixed line-of-sight beam orientation are presented together with the wind velocity measurements by the sonic anemometers.

Figure 5 shows the radial wind velocity observed by the WindCube 100S in the LOS mode, at the azimuth angle of 39° and the elevation angle of 1.8°corresponding to the lidar-beam being oriented perpendicular to the bridge axis, pointing towards the middle of the bridge span. The data acquired at the sampling frequency of 1Hz are seen to capture the main time and length scales of gustiness. The flow obstacle presented by the bridge girder (and/or cables) is clearly visible in the measurements. Downstream of the bridge, some of the data are omitted due to the high noise to signal ratios, corresponding to the carrier to noise ratio (CNR) lower than -27 dB in this case. The significant influence of the terrain on the (radial) wind velocity is notable, including an increase in the velocity with the distance (and an increasing height) from the pulsed lidar. The prevailing wind direction observed by the sonic anemometers was from South (190°).

From the whole family of time-series of the wind speed projected along the pulsed lidars line-of-sight, the wind speed measurements 30 m in front of the bridge structure will be assumed to be generally unaffected by the presence of the 12 m wide bridge deck. These measurements have been singled out and are presented in Figure 6.
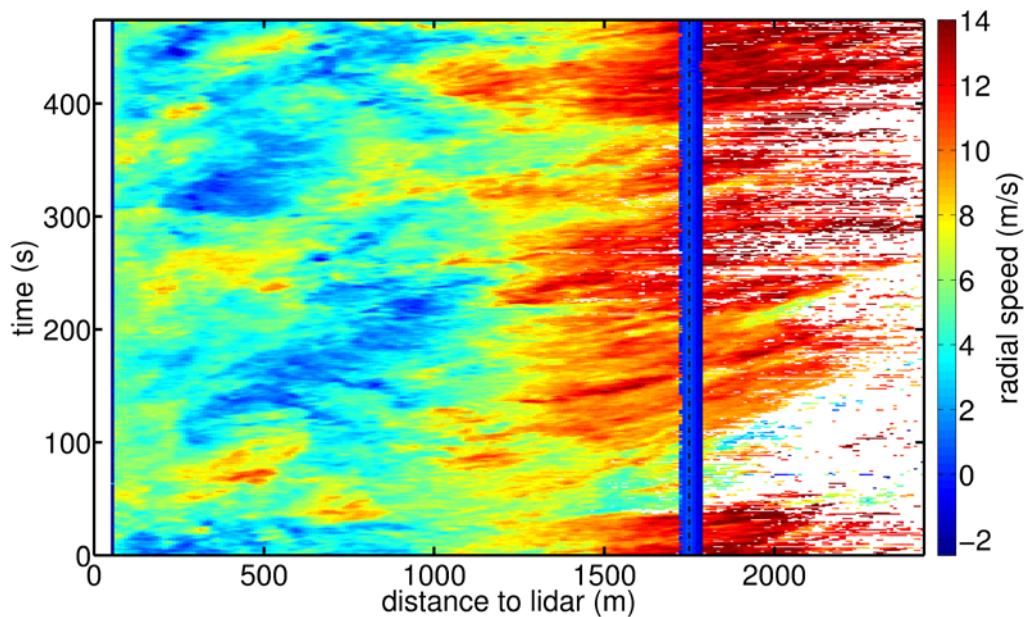

Figure 5. Line-of-sight wind velocity normal to the bridge recorded by the WindCube 100S in the LOS scan on 22.05.2014 starting at 16:12:06.

The data are compared to the corresponding velocity projection obtained from the sonic anemometer in the middle of the bridge span, at hanger H-18. Because of the relatively small elevation angle (1.8°), the displayed wind speed from the sonic anemometer is actually within the horizontal plane, in which the simultaneous data also were recorded by the short-range WindScanners. Again, the velocity component normal to the bridge, V_x, was acquired by the R2D3 WindScanner unit (see Figure 4), where the laser beam had been pointed in the direction normal to the bridge axis, and where the lidars focus distance was set to 40 m. As the WindCube 100S and the short-range WindScanner data stem from sounding volumes centered 30 m and 40 m in front of the bridge, they were numerically "synchronized" with the sonic anemometer data on the bridge, utilizing the "travel time" of 3 s and 4 s respectively. With the prevailing wind direction from South, the velocity fluctuations monitored by the WindScanner and the WindCube were "transported" approximately to the middle of the bridge (H-18) and some 34 m further to the North along the bridge span, respectively, during the time-lags in question. Having in mind such a data interpretation, the fact that the monitoring devices are sensing the flow at three very different distances, as well as the fact that the LOS data by the lidars are affected by the 40° deviation from the mean wind direction, the consistency between the three sets of data in Figure 6 is remarkable. The associated mean wind speed and the standard deviations are presented in Table 1. A higher average (radial) velocity monitored by the WindCube 100S may perhaps be attributed to an accumulated effect of factors such as (i) increase in the wind velocity towards the North part of the bridge span, observed by the sonic anemometers, (ii) a non-negligible vertical velocity component and (iii) a non-negligible effect of the bridge structure.
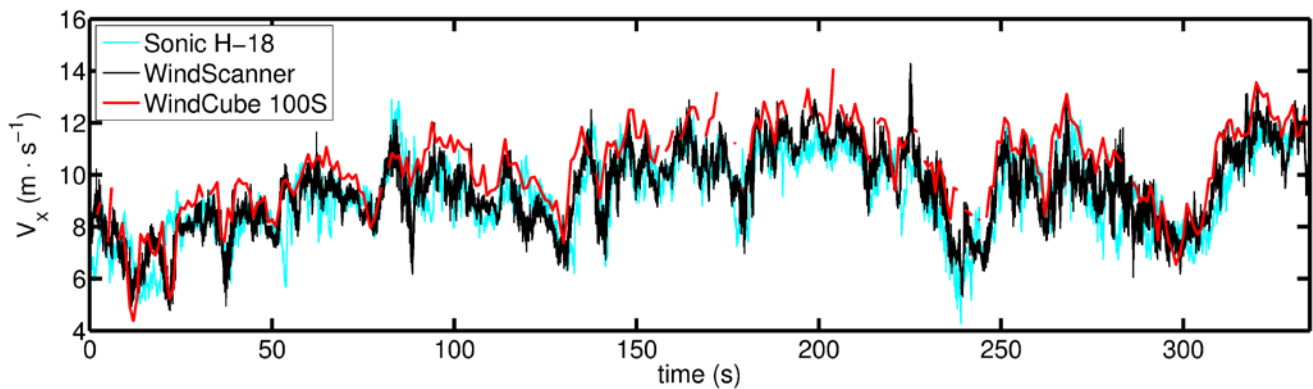

Figure 6. Wind speed normal to the bridge span measured by the long-range pulsed lidar, a short-range cw lidar and a bridge-mounted sonic anemometer on 22.5.2014 starting from 16:13:24

Table 1. Basic statistics of the wind velocity data presented in Fig. 6

Sensors	Mean speed (m/s)	RMS radial speed (m/s)
WindCube 100S	10.3	1.7
Short-range WindScanner	9.4	1.5
Anemometer at H-18	9.2	1.5

In Figure 7 the auto-covariance functions of the wind speeds is presented, for the data displayed in Figure 6. The associated "length scale" of the wind velocity component normal to the bridge axis is around 120 m, deduced from the observed time-lag constant of the covariance equal to exp(-1) and a mean velocity of 9.4 m/s.

During the measurements presented in Figure 6, the R2D1 WindScanner (see Figure 4) was targeting the same "point" 40 m from the bridge as the R2D3, i.e. with the LOS of R2D1 orientated 24° from the bridge axis corresponding to an offset of about 25° from the prevailing wind direction. The effect of the angle between the mean wind direction and that of the lidars LOS on the fine structure turbulence monitored along the fixed line have earlier been investigated in [10]. From combination of the two WindScanners LOS measurements, the wind component pointing in the direction along the bridge, V_y, could also be resolved. Figure 8 presents an inter comparison between the V_y velocity components measured by the two WindScanners 40 m in front of the bridge and the sonic anemometer H-18.
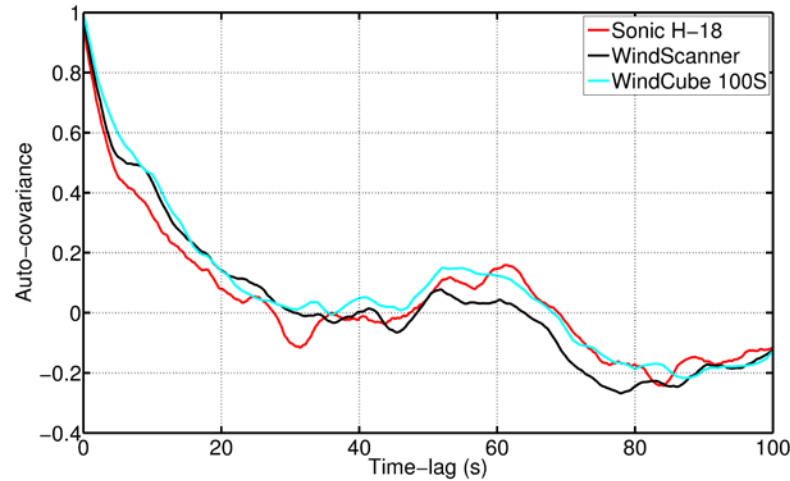
Figure 7.   Auto-covariance function of the horizontal wind speed component normal to the bridge calculated from the data presented in Figure 6.
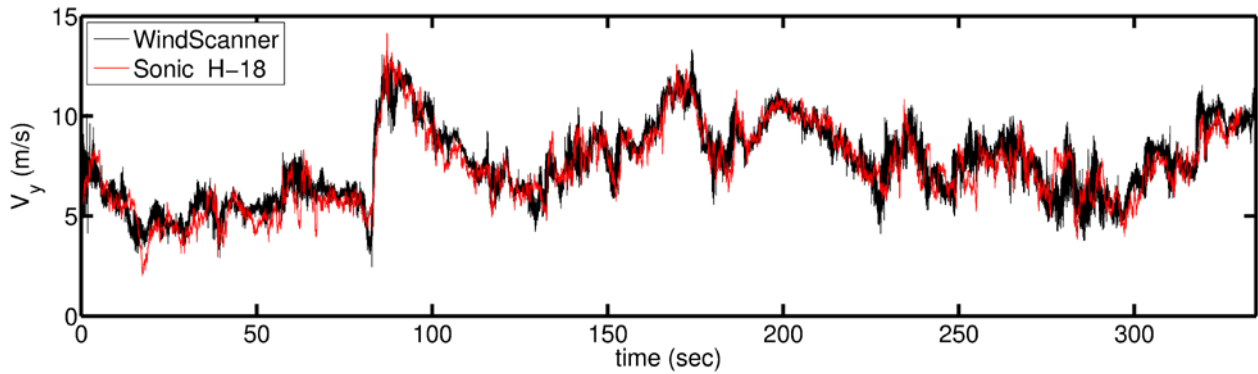

Figure 8. Horizontal wind speed along the bridge axis measured by the WindScanners and the sonic anemometer on 22.5.2014 starting from 16:13:24

3.2   Turbulence characteristics observed by lidars in a "dynamic" scanning mode

In the following, the wind variation along the bridge span is addressed. In Figure 9, the horizontal wind component normal to the bridge, retrieved from the WindScanners data at the 40 m distance in front of the bridge (cf. Figure 4) is presented for a three minutes sampling period. An expanded view of the first half minute is shown in Figure 10, together with the two short-range wind scanners synchronized scan pattern. The figures portray well the large, coherent turbulence structures and their time-scales. A delayed arrival of the large wind gusts on the North part of the bridge (positive y-values in the figures) stems from the prevailing wind direction, from South.
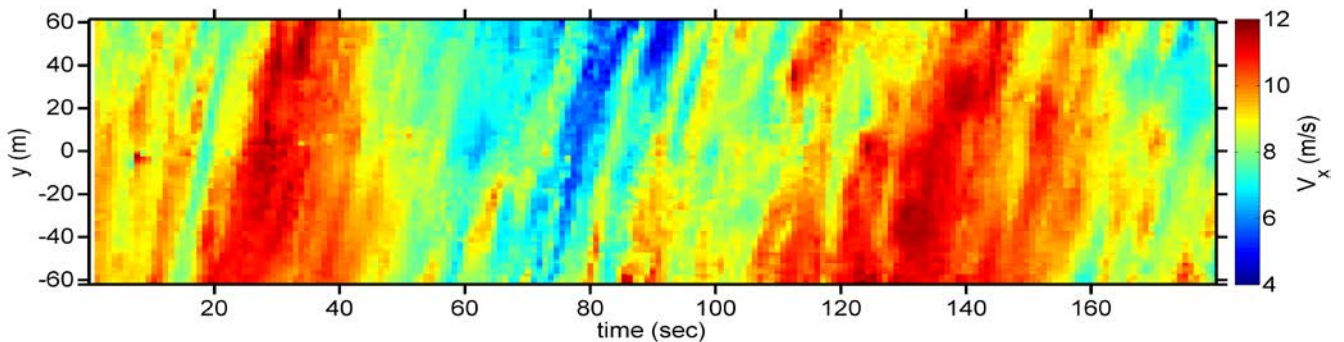

Figure 9. Short-range WindScanner measurements of the horizontal wind component normal to the bridge recorded on 22.5.2014, starting at 17:20.
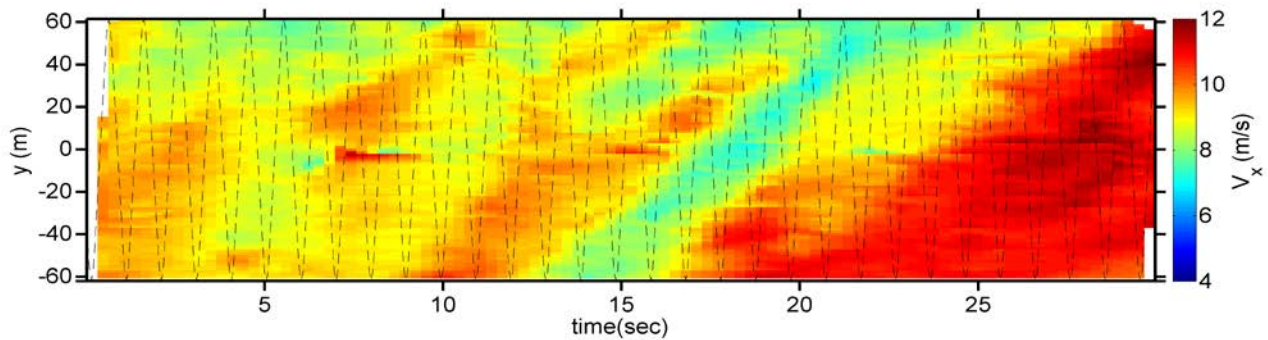
Figure 10. Horizontal wind component perpendicular to the bridge recorded on 22.5.2014, starting at 17:20 (as in Figure 9) and the scanning pattern (dashed).

A similar portrait of the wind field over a larger but coarser scanning grid is displayed in Figure 11, in terms of the LOS projected velocities recorded by the WindCube 100S, at elevations of 1.8° and 3.2°. The comparison between the two PPI records reflects an average LOS wind speed increase with an increasing elevation. The radial projected wind speeds observed at 1.8° include the measurement disturbances by the bridge deck and the two towers. The scanning capture the effect of the fjord topography, including the effect of the "contraction" spanned by the bridge.

In Fig. 12, the coherent structures in the bridge normal wind component upstream of the bridge are investigated in terms the cross-correlation coefficient as function of transverse separation between sampling points. The WindCube 100S velocity data analyzed are from cells at tangential distances of 0 m, 60 m, 90 m, 120 m and 180 m, measured from the 37° azimuth angle pointing towards the bridge hanger nr. 10, a spacing similar to that of sonic anemometers (see section 2.1). As in Figure 11, the center of the pulsed lidars range gate measurement volume is 30 m upstream of the bridge. The correlation coefficient based on the sonic anemometers data is also given in Figure 12, as well as the exponential curves fitted to the coefficients in the least square manner. The correlation decays slower for the lidar measurements in comparison to that of the sonic measurements. This is due to the larger sampling volume of the lidar, which averages out the smaller, uncorrelated eddies. The PPI lidar data studied were recorded with a sampling interval as long as 80 s, in a sequence including several different scanning modes. Consequently, the cross-correlation coefficients based on such a coarse time interval shows a large scatter. The scatter is expected to reduce if a dedicated PPI scanning sequence, with a shorter scanning pattern repetition time, is adopted.
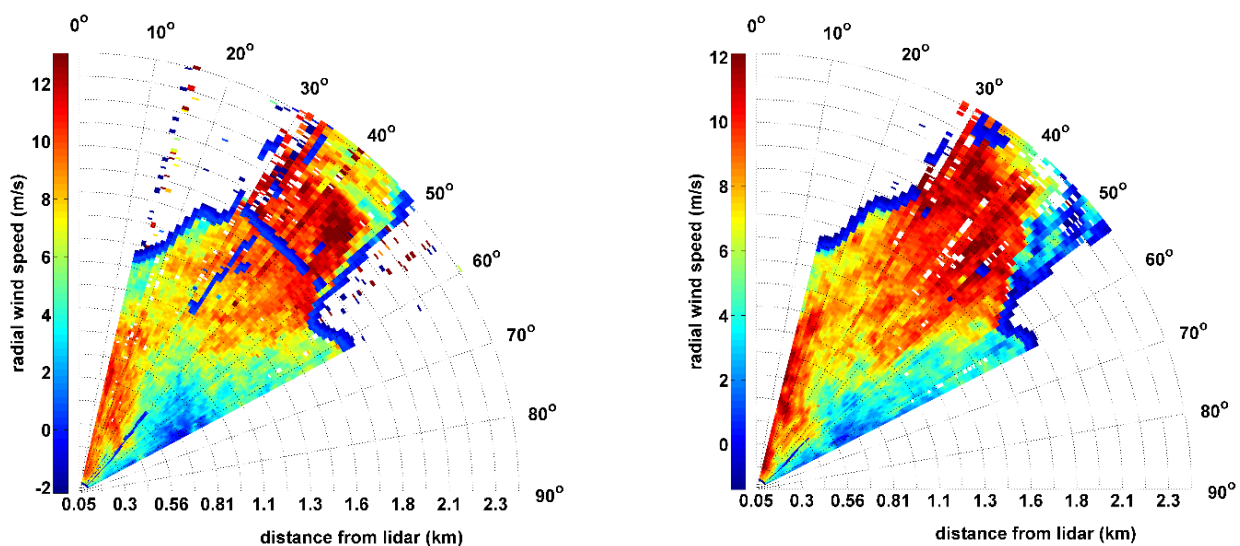

Figure 11. Plan Position Indicator (PPI) mode data recorded at 17:19:23, 22.5.2014, at the elevation of 1.8° (left) and 3.2° (right)
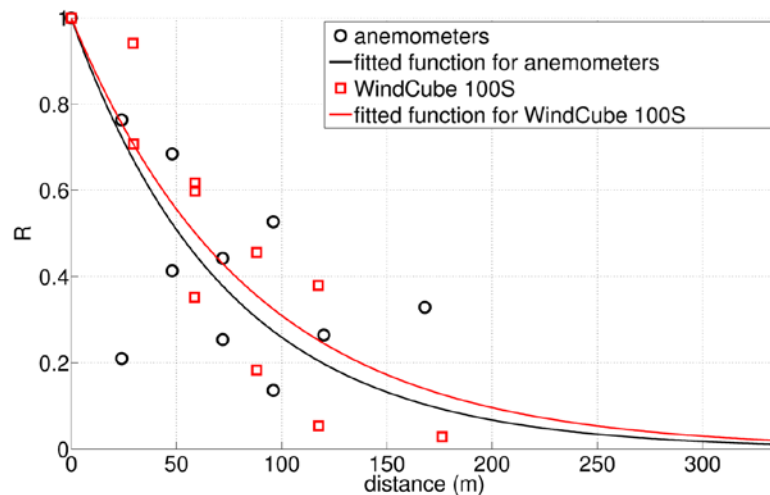
Fig 12. Cross-correlation coefficient for the velocity component normal to the bridge as a function of transverse separation along the bridge deck, 18:15 to 18:25, 22.05.2014.

The line-of-sight wind speeds recorded by the two space and time synchronized WindScanners R2D1 and R2D3 are further utilized to study turbulence and wind fluctuations along the mean wind direction u and normal to it, v. Figure 13 displays the power spectral densities of the two velocity components (u, v) calculated from the LOS measurements from the two cw WindScanners and the sonic anemometer. The spectral values $F_i(k_1)$, $i = u, v$, are given as functions of the wave number $k_1=2\pi \cdot f/U$ and presented in terms of wavenumber pre-multiplied quantities, $k_1*F_i(k_1)$. The WindScanner data from the entire 120 m focus line (see Figure 4), have been divided into 5 m wide cell bins, which are spectrally analysed and then averaged over all bins. The sonic anemometer spectra have been calculated by averaging together the results for the five sonic anemometers described in section 2.1. Data acquired over a 20 minutes long period are analyzed. The analysis was performed by dividing the 20-min time series into blocks of 10-min data, and then ensemble averaging the results for the two periods. The pairs of the spectra agree very well. For wave numbers higher than approximately 0.02, the effects of low-pass filtering due to LOS spatial averaging by the WindScanners is notable, as expected [10].
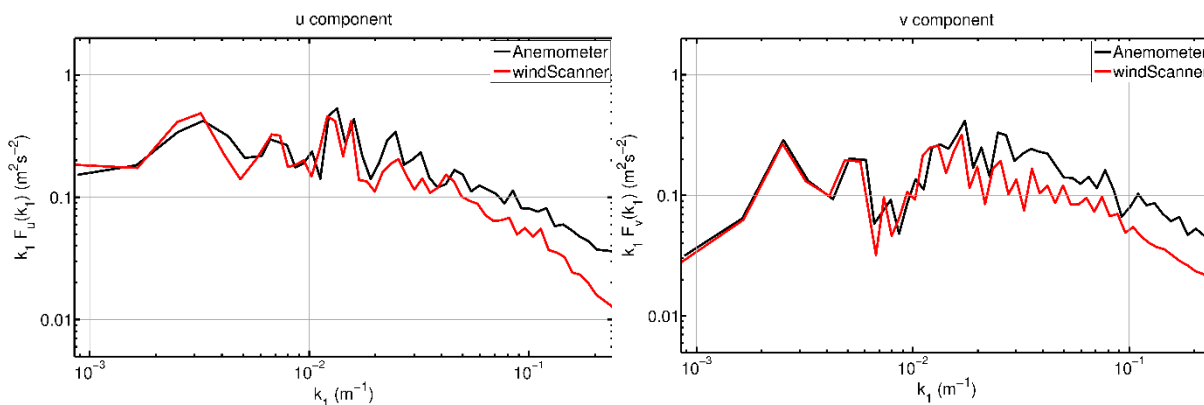

Figure 13: Power spectral density of the longitudinal (left) and transverse turbulence (right) components, based on a 20-min sampling period starting at 17:20, 22.5.2014.

The spatial characteristics of the measured turbulence are furthermore studied in terms of the normalized cross-spectral density functions. The squared coherences of the u- and v-velocity components retrieved from the WindScanners data are presented in Figure 14, as functions of the product between the wave number and the transverse projection of the distances between the measurement points. The time-period studied is as for Figure 12, extended to a total duration of 30 minutes. For the longitudinal wind component, the coherences for different separations D more or less "collapse" into a single curve, indicating relatively large length scales. The coherence functions for the transverse turbulence component show more scatter. The corresponding results based on the twenty minutes long records by the sonic anemometers, for the time period discussed in Figure 13 are also displayed,

in Figure 15. The two sets of the coherence are consistent. It should be recalled that the center of the measurement points surveyed by the two types of instruments are more than 40 m apart and also that the LOS FWHM filter function size varies with range distance in case of the WindScanners data. Also, the bridge deck and the cables might influence the sonic anemometer records to a larger degree than the WindScanners data.
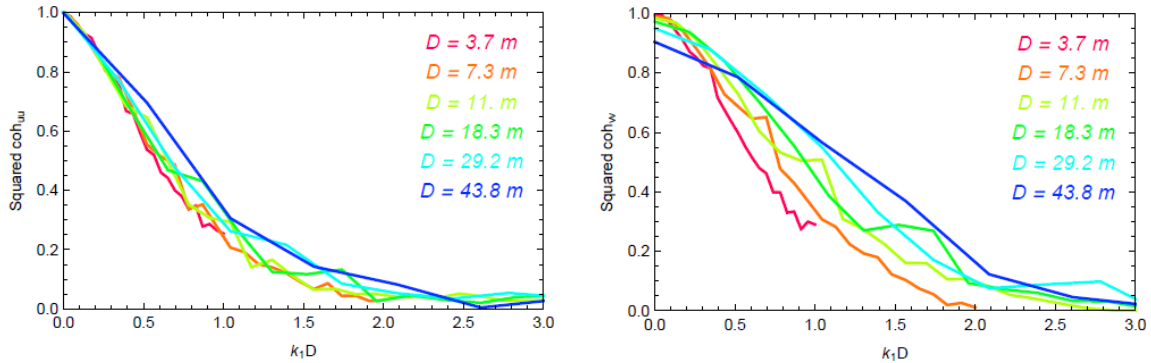

Figure 14. Squared coherence based on the WindScanners data for the along-wind turbulence (left)
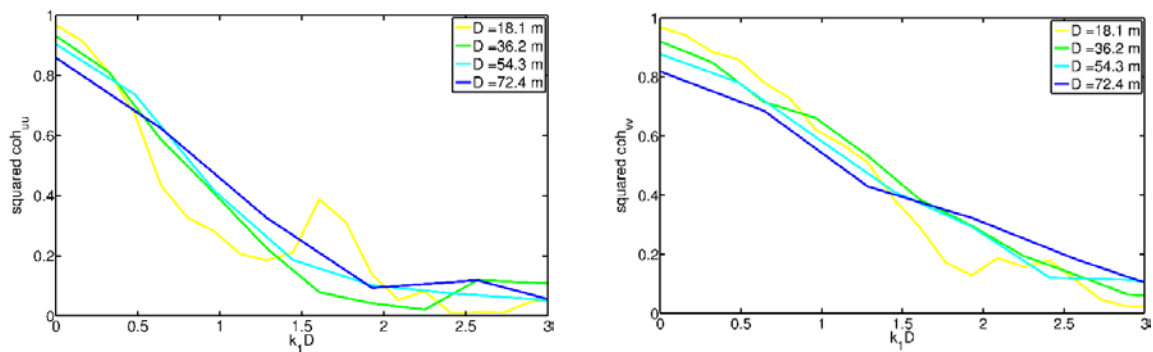and the transverse turbulence component (right)

Figure 15. Squared coherence based on the sonic anemometer data for the along-wind turbulence (left) and
the transverse turbulence component (right).

3   SUMMARY AND CONCLUSIONS

The paper presents a novel application of lidars for wind characterization in bridge engineering, using the Lysefjord Bridge for a case study. Both a long-range pulsed Doppler lidar and a pair of short-range continuous-wave WindScanner lidars were deployed, and the acquired wind data discussed with reference to the measurements by sonic anemometers fixed to the bridge.

The long-range lidar enable one to investigate the slowly varying wind conditions over large distances and capture the "large-scale" effects of the local topography on the wind flow. In the fixed, line-of-sight mode, preferably in syncronized, multi-lidar arrangement, long-range lidars can also provide useful data on the turbulence components up to a scanning frequency of 1 Hz, i.e. in the range containing the large, coherent wind gusts. A dedicated scanning PPI pattern may also be applied in order to capture the lateral correlation of turbulence.

In contrast to a relatively low temporal resolution of the long-range lidars, overlooking the large distances, the short-range WindScanners are able to much faster track coherent structures and changes in the wind components within a pre-selected measurement domain and are thus more suitable for studies of the near-bridge fine scale turbulence. In the present paper, the spectral characteristics of the wind components monitored by two continuous wave synchronized short-range WindScanners are demonstrated to be consistent with those observed by sonic anemometers, apart from the low-pass filtering effect of the lidar sampling functions. A further experimental validation of the theoretical filter functions may assist a future improved interpretation of the lidar wind velocity data, in cases where the measurements by sonic anemometers are not feasible.

ACKNOWLEDGMENTS

REFERENCES

[1]   Norwegian Ministry of Transport and Communication, National Transport Plan 2014 – 2023, Meld. St. 26, (2012–2013), Report to Storting (White Paper) Summary.
[2]   T. Mikkelsen, Lidar-based Research and Innovation at DTU Wind Energy – a Review: The Science of Making Torque from Wind 2014, Journal of Physics: Conference Series 524 (2014) 012007.
[3]   Y. Tamura, K. Suda, A. Sasaki, K. Miyashita, Y. Iwatani, T. Maruyama, K. Hibi, R. Ishibashi, Simultaneous wind measurements over two sites using Doppler sodars, Journal of Wind Engineering an Industrial Aerodynamics 89, 1647–1656, 2001.
[4]   S. Emeis, Vertical wind profiles over an urban area, Meteorologische Zeitschrift 13(5), 353–359, 2004.
[5]   S.E. Lane , J.F. Barlow, C.R. Wood, An assessment of a three-beam Doppler lidar wind profiling method for use in urban areas, Journal of Wind Engineering an Industrial Aerodynamics 11 9(2013) 53-59.
[6]   D.R: Drew, J.F. Barlow, S.F. Lane, Observations of wind speed profiles over Greater London, UK, using a Doppler lidar, Journal of Wind Engineering an Industrial Aerodynamics 121 (2013) 98–105.
[7]   The Norwegian Meteorological Office, Lysefjord Bridge. Suspension Bridge Alternative, Analysis of Extreme Wind Conditions, Rapport No.17/93, 1993 (in Norwegian).
[8]   E. Cheynet, J. B. Jakobsen, J.T. Snæbjörnsson, Buffeting response of a bridge at the inlet of a fjord, Proc. 14th International Conference on Wind Engineering, Porto Alegre, June 21-26, 2015.
[9]   M. Sjöholm, N. Angelou, P. Hansen, K.H. Hansen, T. Mikkelsen, S. Haga, J.A. Silgjerd, and N. Starsmore, Two-Dimensional Rotorcraft Downwash Flow Field Measurements by Lidar-Based Wind Scanners with Agile Beam Steering, Journal of Atmospheric and Oceanic Technology, vol 31, no. 4, pp. 930-937.,10.1175/JTECH-D-13-00010.1, 2014.
[10] L. Kristensen, P. Kirkegaard and T. Mikkelsen, T. Determining the Velocity Fine Structure by a Laser Anemometer with Fixed Orientation; Risø Report; Risø-R-1762, 2011.